

Improved simulation of very heavy rainfall events by incorporating WUDAPT urban land use/land cover in WRF

Pratiman Patel^a, Subhankar Karmakar^{a,b,*}, Subimal Ghosh^{a,c}, Dev Niyogi^d

^a Interdisciplinary Programme in Climate Studies, Indian Institute of Technology, Bombay, India

^b Environmental Science & Engineering Department, Indian Institute of Technology, Bombay, India

^c Department of Civil Engineering, Indian Institute of Technology, Bombay, India

^d Department of Earth, Atmosphere, Planetary and Science, Purdue University, USA

ARTICLE INFO

Keywords:

Local climate zones
WUDAPT
Heavy rainfall
WRF model
Spatial verification

ABSTRACT

A World Urban Data Analysis and Portal Tool (WUDAPT) based Local Climate Zone (LCZ) classification and mapping is done for Mumbai, India. Prior WUDAPT-based urban studies have primarily focused on urban heat island (UHI) assessment, and this is the first study to assess the impact on rainfall simulations. Accordingly, in this study, the impact of incorporating the LCZ map in the Weather Research and Forecasting (WRF) model for simulating very heavy rainfall events over Mumbai is assessed. The classified LCZ map is incorporated in the WRF model, and the model performance is compared against the Control, for four recent very heavy rain events. Comparing the results from paired simulations reveals that the rainfall amount and spatial variability is significantly different when the LCZ framework is used. Implementation of WUDAPT data, introduces heterogeneity in the morphological characteristics of the city, which contributes to microscale feedbacks that appear to organize and impact the mesoscale convergence/divergence and convection fields in the WRF model. The study results show variability within the cases highlighting the need for additional investigations in different cities. Overall, the incorporation of WUDAPT LCZs in WRF results in notably improving the model performance for heavy rainfall simulation in urban areas.

1. Introduction

Urban areas are increasingly vulnerable to climatic extremes such as heat stress, and floods (UN, 2018). The climatic impacts of urbanization are a function of form and morphology, often represented through (i) fraction of impervious area, (ii) thermal and radiative feedbacks of infrastructure such as road, and buildings, as well as local vegetation, and (iii) anthropogenic activities. From the meteorological model perspective, urban land use/land cover (LULC) classification seeks to capture the different urban form and morphological features. The urban classification within the coupled model then provides the parameters that form the basis for energy partitioning, and through the land-atmospheric coupling affects boundary layer evolution and mesoscale feedbacks.

In the majority of contemporary meteorological models, such as the Weather Research Forecast (WRF) modeling system, or the Regional Atmospheric Modeling System (RAMS), the urban LULC typically consists of one to three urban classes (Chen et al., 2011). It is recognized that the urban classification is more heterogeneous than the three urban categories (residential, mixed residential, and commercial/industrial), and efforts are underway to incorporate more detailed urban morphological information into the

* Corresponding author at: IDP in Climate Studies, Indian Institute of Technology, Bombay, India.

E-mail address: skarmakar@iitb.ac.in (S. Karmakar).

atmospheric models. Some of the earlier community efforts included the CORINE LULC for European region (Bossard et al., 2000), and the National Urban Database and Access Portal Tools for the USA (Glotfelty et al., 2013). More recently, one collaborative activity underway that is gaining increasing popularity is through the World Urban Database and Access Portal Tools (WUDAPT) (Ching et al., 2018).

The WUDAPT framework builds off the Local Climate Zones (LCZ) mapping that classifies the urban landscape into 17 different categories (Stewart and Oke, 2012). The LCZ classification considers 10 classes (LCZ 1–10) for built-up areas, and 7 classes (LCZ A–G) for vegetation, soil, sand, rock, and water. The major components of the LCZ classification are the height of the buildings, the distance between the buildings, nearby surface cover, and thermal properties of the building materials.

To derive LCZs, different methods have been proposed. Examples include, using SAR and multi-spectral datasets (Bechtel and Daneke, 2012; Bechtel et al., 2016; Xu et al., 2017; Wittke et al., 2017), GIS models (Gál et al., 2015; Geletič and Lehnert, 2016; Wang et al., 2018), contextual classifier (Verdonck et al., 2017), ensemble learning (Yokoya et al., 2017), hyperspectral and LiDAR dataset (Bartesaghi Koc et al., 2017), and OpenStreet Maps data (Samsonov and Trigub, 2017). Amongst these, the method proposed by Verdonck et al. (2017) has (i) a relatively straightforward workflow, (ii) less computational needs, and (iii) provision to use open source software and datasets. The method requires the pre-processing of Landsat imagery with a moving window, and random forest classifier for supervised classification using datasets provided by a local expert.

The WUDAPT/LCZs framework has been used in various observational and model-based synthesis studies. The majority of these studies have focused on analysis of temperature changes (e.g. Leconte et al. (2015); Cai et al. (2017), and in some cases for climate modeling (Feddeema et al., 2015); and broader environmental studies (Thomas et al., 2014; Feddeema et al., 2015; Verdonck et al., 2017; Cai et al., 2017; Ching et al., 2018). Brousse et al. (2016) used a WUDAPT LCZ dataset in WRF model over Madrid, Spain and showed a positive impact on temperature simulations for different LCZs. Similarly, Kaloustian and Bechtel (2016) generated the LCZs for Beirut, Lebanon and incorporated it into the Town Energy Balance (TEB) model to calculate the roof and canyon temperature with the energy requirement for cooling. A recent study by Brousse et al. (2019) mapped LCZs over sub-Saharan African cities of Kampala, Uganda, and Dakar, Senegal, and integrated it with the offline climate model (TERRA-URB, Wouters et al. (2016)) to help study health aspects. It is clear from the literature that there have been very few studies WUDAPT based over Indian regions (e.g. Niyogi (2017); Kotharkar and Bagade (2018)). Moreover, no previous study has assessed the impacts of LCZs on heavy rainfall over urban areas.

This study, thus, provides one of the first assessments of the impact of considering the WUDAPT LCZs on the simulation of urban rainfall. The key research objective is to investigate the influence of detailed urban land use/land cover information on simulations of very heavy urban rainfall.

2. Experimental setup

The study domain covers Mumbai, which is a coastal megacity in India. The LCZs were developed for the city using the WUDAPT methodology (Verdonck et al., 2017). The LCZ map was evaluated by local experts by visiting the different representative locations and taking photographs across the city. The evaluated LCZs were implemented in the WRF model, and simulations are performed using default land use/land cover as Control run and LCZs as WUDAPT run. An object-based comparison between Control and WUDAPT simulation was done for a very heavy rainfall event that occurred on 29 August 2017; this was followed by assessments for three additional very heavy rain events: 16 Jun 2013, 15 Jul 2014, and 18 Jun 2015.

The study area, along with the details of the urban classification methodology is discussed next. This is followed by the summary of a representative, very heavy rain case (29 August 2017). The three additional very heavy rain cases are also simulated for 14 June – 17 June 2013, 14 July – 17 July 2014, and 17 June – 22 June 2015, but not discussed in detail. Each of these events had a relatively similar synoptic setup in which, (i) an active southwest monsoon had set in over western India, and (ii) an intense low pressure monsoon trough spanned from southern India to north of Mumbai along Gujarat coast, and interior regions.

The WRF model setup, the observational datasets, and model evaluation methodology are also outlined ahead. Note that the reference to 'very heavy' rain event follows the classification adopted by the India Meteorological Department (IMD), which considers the rainfall threshold of 124.5 mm for a 24 hour period (IMD, 2019a).

3. Study area

Mumbai is located on the west coast of India. As of 2014, the city covers an area of 705 km², with a population of nearly 20 million (Angel et al., 2015). Mumbai receives an annual rainfall of 2373 mm of which more than 95% is during monsoon months from June through September (IMD, 2019b). The location of the city with complex terrain (Western Ghats) and coastal setting makes it vulnerable to monsoon rains, storm surges, and frequent flooding (Dhiman et al., 2019).

One of the interesting features of the heavy rains over Mumbai is the large spatial variability across the city. This variability poses a challenge for accurate rain forecasts and flood warning studies as well as local disaster management efforts. As an example, one of the well-studied heavy rain events is the 26 July 2005 rainfall over Mumbai (Jenamani et al., 2006; Vaidya and Kulkarni, 2007; Kumar et al., 2008; Lei et al., 2008; Chang et al., 2009), which recorded over 944 mm in the western parts of the city (Santacruz) and only 73 mm of rain in the southern Mumbai observatory (Colaba) that was at a distance of about 25 km.

The study area over Mumbai has a heterogenous landuse with burgeoning residential, commercial regions, and notable socio-economic contrasts with transient housing (slums), as well as tall, concrete buildings. Mumbai is considered the economic capital of India and the heavy rains cause a cascading impact on the region's socioeconomic fiber.

4. LCZ classification

Landsat 8 imagery was downloaded for a domain that encompassed the broader Mumbai area. The domain covered 72.69° to 73.29° longitude and 18.79° to 19.58° latitude. A total of five Landsat 8 imagery (06 Jan 2014, 23 Feb 2014, 12 Apr 2014, 06 Nov 2014, and 08 Dec 2014) were used. The spectral information from open-source Landsat 8 data was used in which the bands 8 (panchromatic) and 9 (cirrus) was not incorporated following Bechtel et al. (2015). A moving window was applied over each band to integrate contextual information. The moving windows include neighborhood pixel information, which increases the overall accuracy of the LCZ map (Verdonck et al., 2017). The bands were resampled from 30 m to 100 m before using further in the classification process. The training datasets were derived in the form of KML files from Google Earth with the help of local experts. The information from the training and Landsat imagery was used in supervised classification using random forest algorithms in SAGA platform (Conrad et al., 2015).

Fig. 1 shows the LCZ map for Mumbai. From the map, LCZ 1–3 are found in the south and central part of Mumbai, while LCZ 4–6 are in the outskirts. LCZ 7 is concentrated in regions with transition housing (slums), and several clusters of LCZ 7 are located across the city. LCZ 8 and 10 are located primarily in the eastern and northern parts, while LCZ 9 is located in the northernmost part of the city. LCZ A–C is found along a reserve/national park, and also along the protected coastline.

The classified LCZ maps were evaluated further by at least two local experts who made site visits to different locations across the city. The experts visited locations for each of the LCZ, took onsite pictures, and conducted their assessment regarding the LCZ classification. Fig. 2 shows an example of one of the subregions in central Mumbai, which has a cluster of different LCZs and the corresponding onsite pictures that were used for the evaluation.

Using the onsite expert input and the SAGA based classification, an accuracy assessment was performed to assess ‘overall accuracy’. This was defined as the ratio of number of correctly classified pixels to the total number of pixels. The assessment yielded an ‘overall accuracy’ of 86%, and the corresponding ‘confusion matrix’ is provided in the supplementary information (Story and Congalton, 1986).

5. The 29 August 2017 very heavy rain event

Mumbai receives most of the rainfall during the active phase of southwest monsoon. During July and August, the strong, moisture-rich westerlies from the Arabian Sea are orographically lifted due to the Western Ghats, causing heavy rainfall over the west coast of India (Grossman and Durran, 1984). The 00Z (0530 LT) 28 Aug 2017 analysis identified a well-marked, low-pressure region (depression) that generated over the Bay of Bengal and extended considerably inland over eastern and central India. There was also a Mid-Tropospheric Cyclonic (MTC) circulation present over Gujarat (north of Mumbai) and west coast (near Mumbai) that contributed to shifting the monsoon depression inland. The 00Z 29 Aug 2017 analysis showed an active monsoon trough that moved from the Arabian Sea towards the west coast affecting the region over Mumbai. The presence of the MTC north of Mumbai and the westward-moving low-pressure area from the east led to convergence over Mumbai. This synoptic setting formed the stage for very heavy rains over the Mumbai region. On 29 Aug 2017, Mumbai officially received 252 mm. The southern Mumbai region (Colaba) received 138 mm while about 15 km north, the central Mumbai (Dadar) area received 353 mm of rain.

6. WRF model configuration

Model simulations were performed using the WRF mesoscale modeling system (Skamarock et al., 2008). The Advanced Research WRF (ARW) version 3.9.1.1 was used. The WRF model has been used in several quasi-operational as well as process-based assessments of heavy rain simulations for the Indian monsoon region (Rao et al., 2007; Kumar et al., 2008; Routray et al., 2010; Chawla et al., 2018; Dutta et al., 2019).

The WRF domain was configured with three nested grids with 38 vertical levels spanning a log-linear spacing. The lowest model level was 25 m from the surface, and 23 levels were within the lower 5 km to capture the boundary layer and mesoscale convective processes that are typically active over the region. The domain was set with 9 km (163×141), 3 km (316×295), and 1 km (352×352) horizontal grid spacing covering the Arabian Sea, and west coast, and telescopically centered on the Mumbai region (Fig. 3(a)).

The experimental setup consisted of setting the model simulations with a Control and WUDAPT urban landcover. The Control considers the default WRF/Noah land cover derived from MODIS fields, while the WUDAPT run considered additional 10 classes of Landsat-derived, WUDAPT trained, surface fields from the LCZ map that was developed. Fig. 3(b, c) shows the corresponding LULC maps. The urban class (shown in white colour) in Control simulation is further divided into ten different classes in WUDAPT simulation, which represents the heterogeneity within the urban class and a more realistic representation of the landscape (Stewart and Oke, 2012).

This study considered the urban Noah coupled to WRF (Chen et al., 2011; Salamanca and Martilli, 2010) with the multilayer Building Energy Parameterization (BEP) scheme. The urban Noah model is used because (i) it is formulated to better represent the feedbacks from the detailed urban processes over the city-dominated domains, and (ii) to align with the goal of studying the effect of WUDAPT-based urban representation on the coupled model simulations. The BEP model considers a 3-D urban morphology and the associated turbulence and energy balance aspects on the dynamical and thermodynamical features of the built environment. The model accounts for the geometry of the urban area, which is characterized by the building height distributions, building width (B), and street width (W). The urban morphology information was provided using a look-up table for each urban class. The model

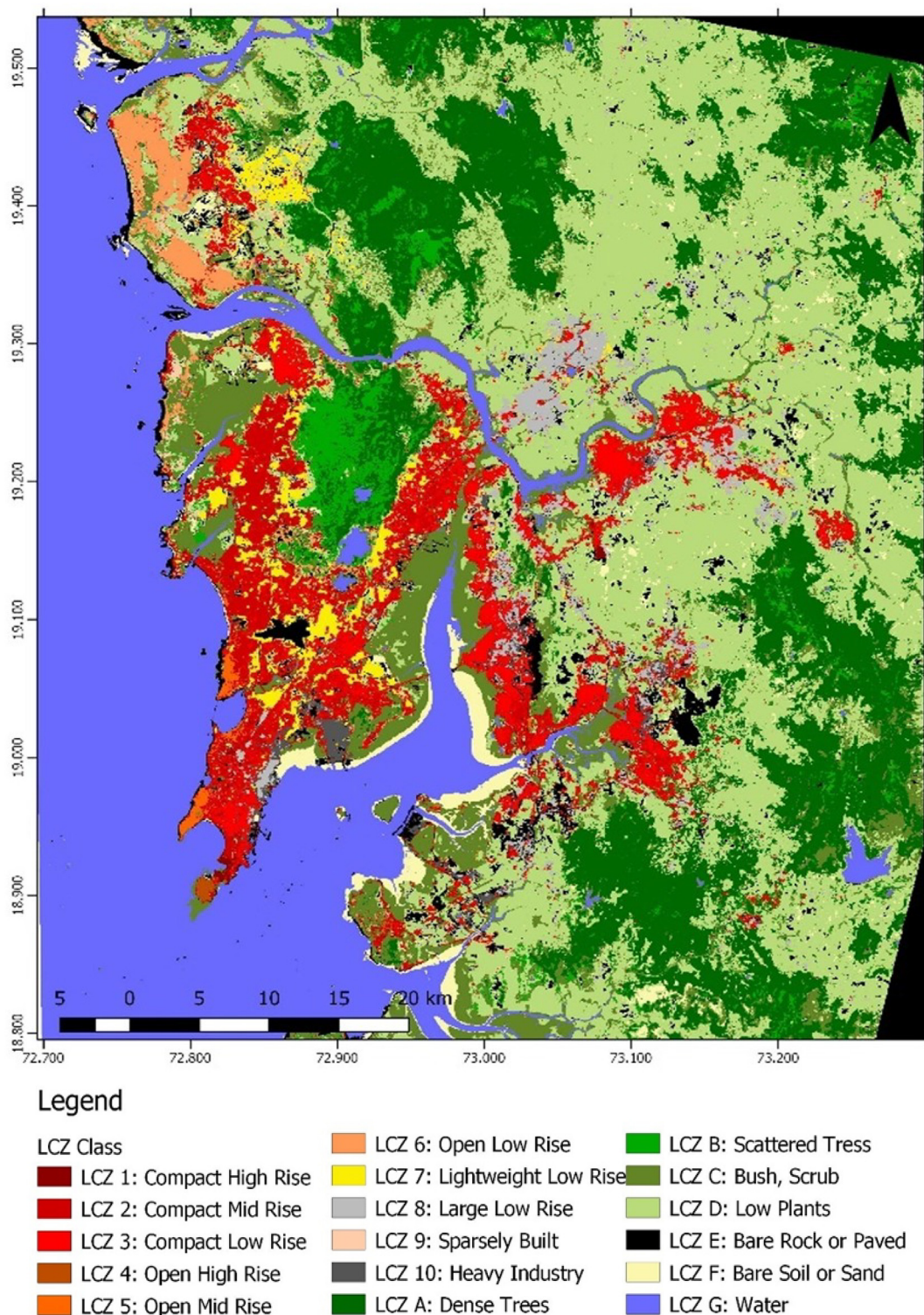


Fig. 1. WUDAPT-based LCZ map of Mumbai, India.

dynamically solves for each time step (taken as 60s in this study) the surface energy balance for roofs, walls, and roads while considering the vertical structure of buildings, and distributes the sources and sinks of heat, momentum, and moisture (Salamanca et al., 2010). The BEP is only run for the urban grids within Noah land model.

An important parameter in BEP through which the energy and momentum exchange is modeled is the turbulence scale length. The

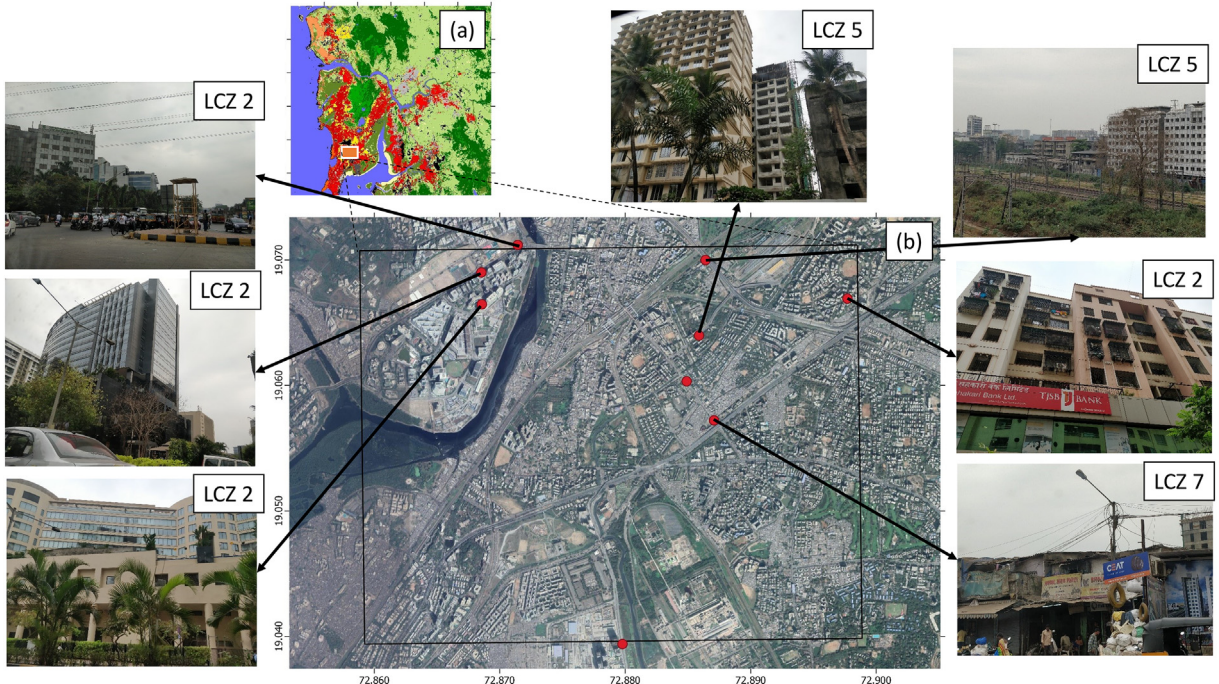


Fig. 2. (a) LCZ across Mumbai showing a subset of an area (shown by the orange box), (b) Google Earth Imagery over the inset and different locations for the photographs, and their corresponding LCZs.

length is the height above ground which is modified to account for the impacts of buildings, for i th level as,

$$\frac{1}{l_{b|I}} = \sum_{iu=ibu}^{nu} \gamma(z_{iu}) \frac{1}{z_{iu}} \quad (1)$$

$$l_{ground|I} = \frac{1}{\left(\frac{W}{B+W}\right) \frac{1}{z_I} + \left(\frac{B}{B+W}\right) \sum_{iu=1}^{ibu-1} \gamma(z_{iu}) \frac{1}{(z_I - z_{iu})}} \quad (2)$$

where ibu is the lowest level of the urban grid, $\gamma(z_{iu})$ is the density of the building of height z , W is the width of the street, B is the width of the building z_{iu} , and z_I is the height above the ground. Eq. (1) is applicable to model levels less than or equal to the height of the buildings (Martilli et al., 2002), that is, for within street canyon features.

The WRF model configuration followed the physical parametrization that has been used over the study domain in prior studies (e.g., Patel et al., 2019). Some of the notable options included Dudhia (1989) shortwave radiation and the Rapid Radiative Transfer Model (Mlawer et al., 1997) for the longwave radiation scheme. Surface energy balance and surface land surface processes were represented using the Noah Land Surface Model (Tewari et al., 2004). The model was run with BouLac (Bougeault and Lacarrere, 1989) planetary boundary layer option that was configured to run with the BEP scheme. Cloud convection and microphysical processes were parameterized following Thompson et al. (2008), and Grell-3D (Grell and Dévényi, 2002). The innermost domain considered explicit convection and did not consider the cumulus parameterization.

The WRF initial and boundary conditions were obtained from the National Centers for Environmental Prediction Final Operational Model Global Tropospheric Analyses (NCEP FNL) data (available at <http://rda.ucar.edu/datasets/ds083.2>) at 6-hourly temporal and 1-degree spatial resolution. The simulations were conducted for 84 h, with the initial 12 h considered for the model spin-up and not used in the synthesis of model results. The same modeling and experimental configuration were maintained for each of the four very heavy rain events simulated in this study.

7. Observational dataset

The observational dataset primarily includes hourly rainfall from 41 Automatic Weather Stations (AWS) obtained from Municipal Corporation of Greater Mumbai. The AWS network-based rainfall is considered representative of the region, and has a sufficient density to capture the rain within the city. The data has also been used in prior, recent studies (Paul et al., 2018; Patel et al., 2019). For spatial distribution of rainfall in urban settings radar based datasets are preferred (Niyogi et al., 2011; Lorenz et al., 2019); however, they were not available for the study domain. As an alternative, remotely sensed product from Global Precipitation Mission (GPM) based, rain gauge merged product: IMERG V05B Final Run is used. This data was available for each of the four events being studied. The IMERG products provided more comprehensive coverage along with half-hourly temporal resolution and about 10 km

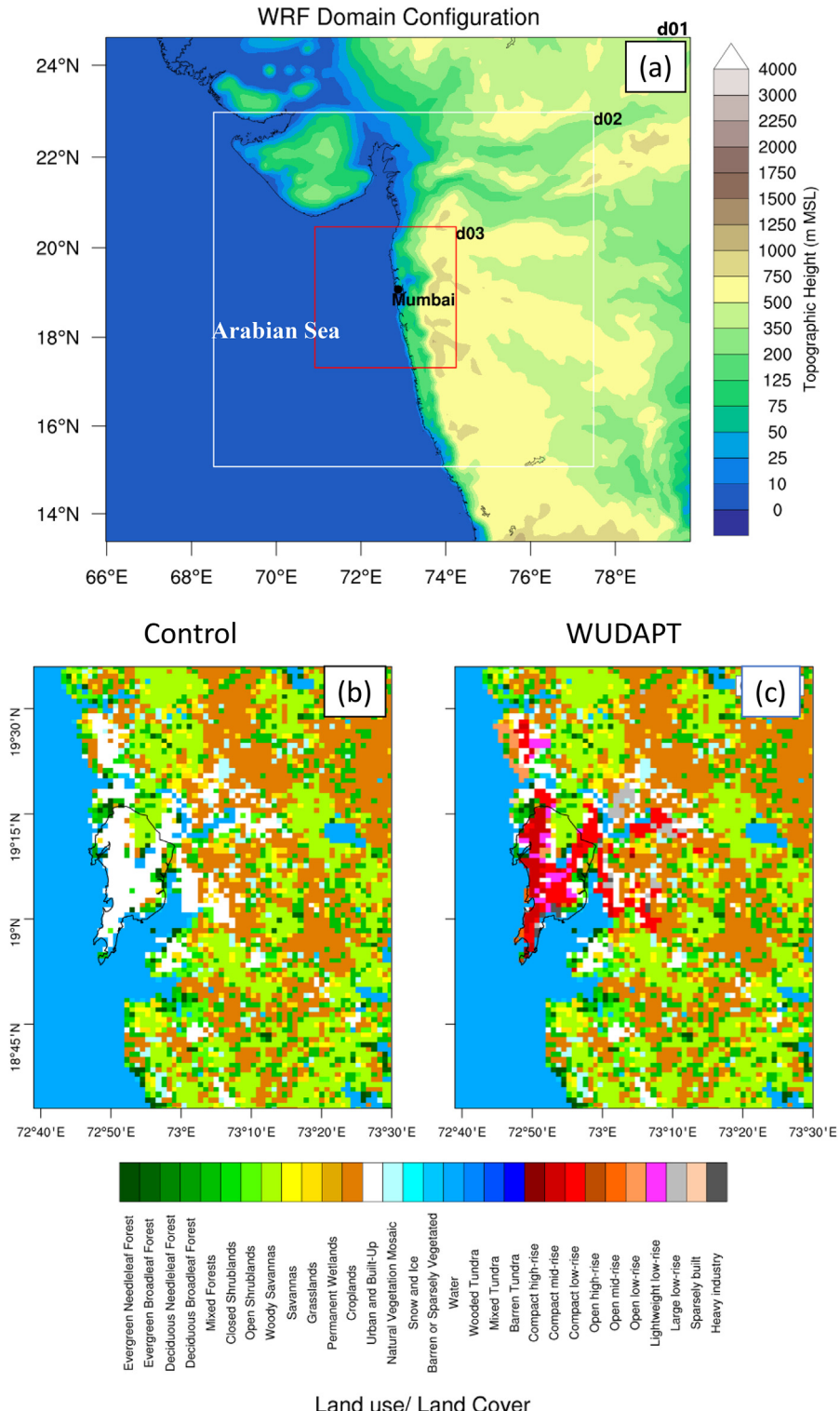


Fig. 3. (a) WRF nested domains with topography. (b) MODIS LULC used in Control simulation. (c) LULC used in WUDAPT simulation. The urbanization features such as mid-rise buildings that are common across Mumbai are notable in the WUDAPT map.

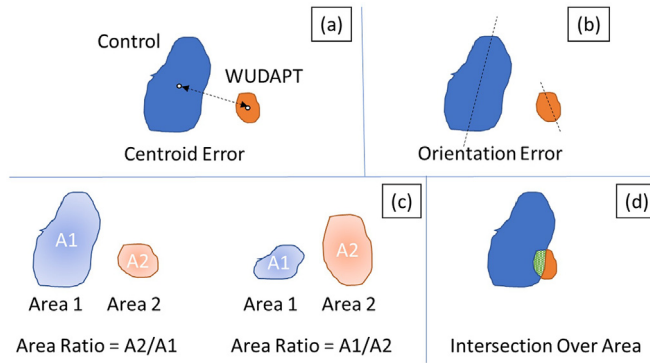


Fig. 4. Illustration of MODE objects and attributes. The Control object is shown in blue, and the WUDAPT object is in orange. (a) Distance between the center of the two objects is centroid error, (b) change in the orientation of the object is the orientation error, (c) the ratio of smaller to a larger area is area ratio, and (d) overlap of area between the two objects is intersection over the area. (For interpretation of the references to colour in this figure legend, the reader is referred to the web version of this article.)

spatial resolution (0.1 deg). The AWS and IMERG V05B Final Run rainfall was resampled from sub-hourly to hourly datasets to match with WRF outputs.

8. Model diagnostics

By nature of the variability and the limited sampling of rainfall in a heterogeneous urban area, the comparison between model runs and observations requires a more sophisticated set of analysis than the traditional comparisons typically reported in the literature. This study adopted the Method for Object-based Diagnostic Evaluation (MODE, Davis et al. (2009)) for assessing the model results (Clark et al., 2014; Cassola et al., 2015). MODE resolves various objects within the data fields (simulated rainfall from the paired runs). For the hourly fields the following five steps were performed: (i) the rainfall data were plotted, (ii) the rainfall fields were passed through a convolution filter, (iii) the fields were masked using a user-defined threshold (rainfall greater than 0.5, 1, 2, 5, 10, 20, 25, 30, and 40 mm). This created the ‘objects’. The objects generated from the Control and the WUDAPT rainfall fields were then (iv) ‘matched’ into a single field, and (v) ‘merged’ into groups. The resulting objects (following steps iv and v) were analyzed using descriptors such as (a) ‘centroid error’ (difference between the distance of the centroid of two fields), (b) ‘orientation error’ (change of angle between the two objects), (c) ‘area ratio’ (the ratio of areas defined by the smaller of the fields relative to the higher), and (d) ‘intersection over area’ (overlap of area between the two objects).

Fig. 4 provides a schematic representation of these MODE attributes, considering the data fields from the Control and WUDAPT runs. In the case of area ratio, a smaller area was selected as a numerator to reduce the likelihood of anomalously high values skewing the results and to scale the values between 0 and 1 for each time step. The area ratio was thus a measure of the difference between the area of the two objects, whereas ‘intersection over area’ represents the area intersected by the two objects. Both the quantities were unitless and range from 0 to 1. A value of 1 for area ratio, indicates no difference between the two areas, while 0 represents the object to be missing from one of the simulations. Similarly, for intersection over the area, 1 shows a perfect match between the two areas, while 0 represents no match between the areas.

9. Results

Fig. 5(a) shows the mean cumulative rainfall from observations and the Control as well as WUDAPT simulations. The observed and the simulated rainfall (from both the runs) were similar upto 04Z 29 August and after 12Z, the model results overestimated the observed. The WUDAPT simulation results showed better agreement with the observed (quantified by a reduced mean error of 55 mm for the WUDAPT compared to 140 mm for the Control). The model rainfall values were also compared against observations at five locations that witnessed highest totals (shown in Fig. 5(b)). As seen in the figure, the Control run significantly overestimated, whereas WUDAPT (blue shade) simulated relatively better rainfall amounts. Interestingly, both the simulations showed overestimation for the five stations.

Fig. 6 shows the total accumulated rainfall over the study area. The WUDAPT simulated rains are lesser than the Control by about 75–150 mm. For the northern coastal part of Mumbai, the Control underpredicted rainfall by 100–130 mm whereas WUDAPT, again yielded a better agreement.

The spatial rainfall variability across the city is shown in Fig. 7 as a box-whisker plot for different LCZs. The overall distribution of WUDAPT rainfall is better than Control with the 25th- and 75th-percentile being closer to observations. Indeed, both the simulations overpredicted the rainfall amount in which the results from the Control run varied from 280 to 785 mm, while that from WUDAPT ranged from 305 to 615 mm. The observations, on the other hand, ranged between 235 and 492 mm. There are some notable extreme values in the WUDAPT rainfall fields, both on the lower and upper bounds (noted by open circles in the box-whisker plot). The extreme (or anomalous) rains simulated in the WUDAPT run is likely due to the spatial variability that was introduced in the urban

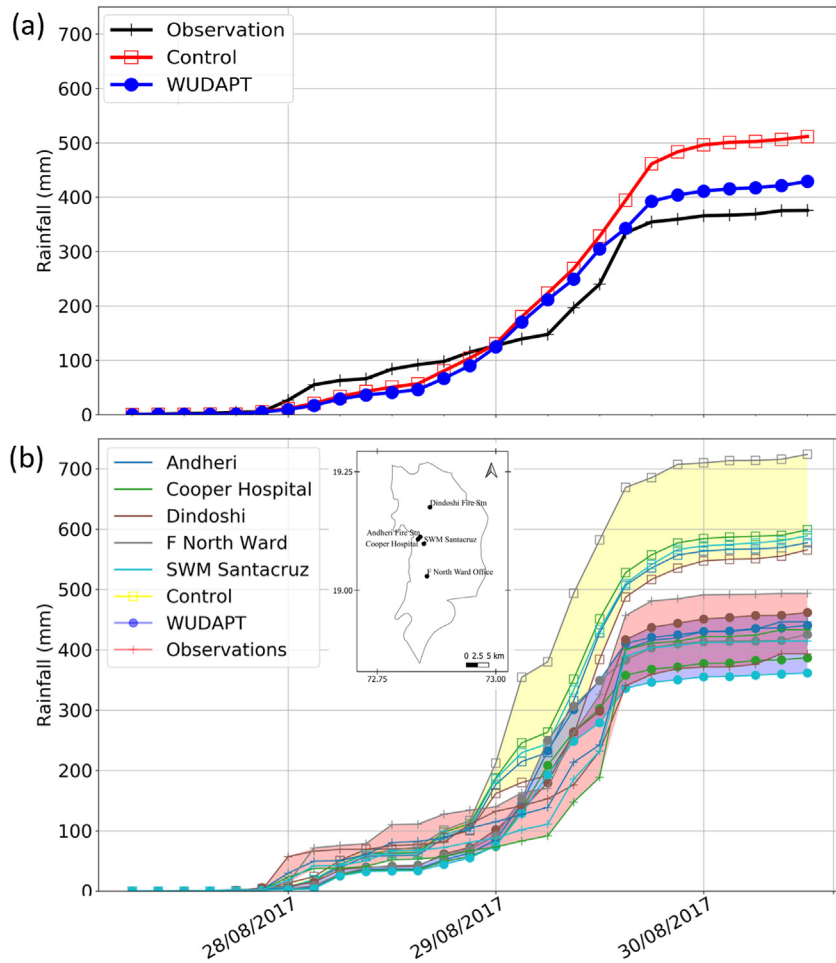


Fig. 5. (a) Cumulative rainfall from observed (green), control (red), and WUDAPT (blue) simulations. (b) Cumulative rainfall from 5 stations that recorded the highest rainfall for the event: Andheri, Cooper Hospital, Dindoshi, F North Ward, and SWM Santacruz, compared with control, WUDAPT, and AWS observations. Yellow band shows the spread of rainfall obtained from Control; similarly, the red band is for the Observations while blue is for WUDAPT. The inset shows the location of the five selected AWS stations. (For interpretation of the references to colour in this figure legend, the reader is referred to the web version of this article.)

morphological fields in the WUDAPT run and is discussed ahead.

Comparing the rainfall distribution for different LCZs, the rainfall in LCZ 2 (Compact Mid Rise) and 3 (Compact Low Rise) varied over a wide range from 300 to 625 mm. On the other hand, LCZ 1 (Compact High Rise) and LCZ 4 (Open High Rise) showed the least variability and was likely also because of the smaller area the two LCZs covered across the domain. The highest rainfall totals were for LCZ 10 (Heavy industry), compared to all other LCZ classes, whereas the smallest rainfall values were simulated over LCZ 4 (Open High Rise). LCZ 9 (Sparsely built) and LCZ 5 (Open Mid Rise) showed lesser variability while LCZ 8 (Large Low Rise), LCZ 7 (Lightweight Low Rise), and LCZ 6 (Open Low Rise), which are 1–3 storied building complexes, show moderately high variability in the simulated rainfall amounts.

Since the model configurations between Control and WUDAPT were identical, and the only change was the urban morphological information, it follows that the rainfall variability is mainly due to the surface-atmosphere interactions within the model. The changes in the vertical wind velocity between the two simulations were reviewed further, to understand the differences in the dynamical forcings. Fig. 8 shows an illustrative snapshot corresponding to the afternoon condition (for 1430 LT 28 August). The simulated vertical velocities provide an insight into the atmospheric instability, and the locations of the intense updrafts- downdrafts is often a seat of micro/meso-convective activity. The accumulated rainfall from the Control simulations was around 600 mm between the 72.88° and 73.07° E, and the WUDAPT simulation redistributed the rainfall from 375 to 500 mm over the same region. As a result, the vertical winds for that particular cross-section was reviewed further. The region of positive vertical velocities found in the Control simulation between 72.65° to 72.90° E was rearranged in the WUDAPT simulation with a strong, localized convergence likely around 800 mb level between 72.69° to 72.88° E, leading to a surface updraft – downdraft - updraft zone over a relatively narrow region. Interestingly, this locale also corresponded to the peak rainfall in the WUDAPT run. The Control simulation showed a much wider area of strong updrafts followed by a similar broader area dominated by downdrafts. This likely translates into a much more

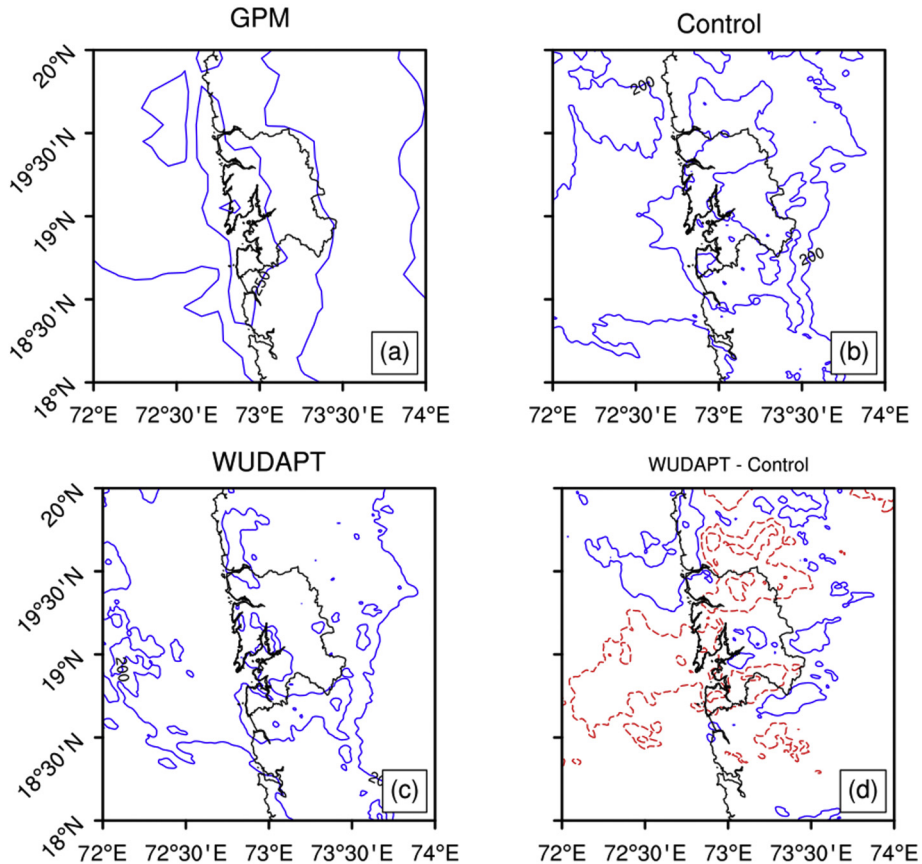


Fig. 6. (a–c) Total accumulated rainfall (mm) from GPM/IMERG observations, Control, and WUDAPT simulations. (d) Difference between WUDAPT and Control.

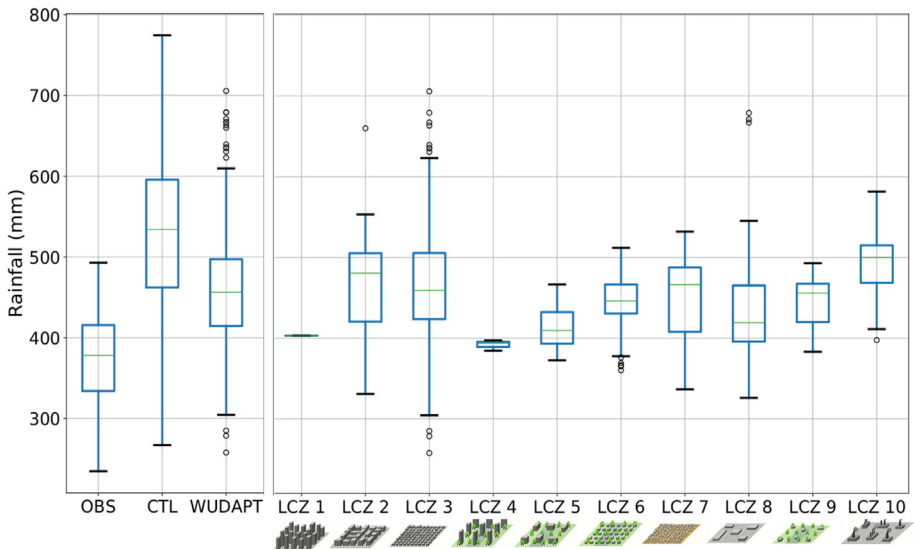


Fig. 7. Box-whisker plot showing accumulated rainfall for observed (OBS), Control (CTL), WUDAPT, and LCZ 1–10. The representative illustration of LCZs is adapted from [Stewart and Oke \(2012\)](#).

coherently organized convective region predicting sustained heavy rains compared to the WUDAPT run.

The changes in the surface atmospheric stability in the two model runs is considered as a result of additional urban morphological information available through WUDAPT for building height, street width, roughness height, and turbulence estimates (outlined in

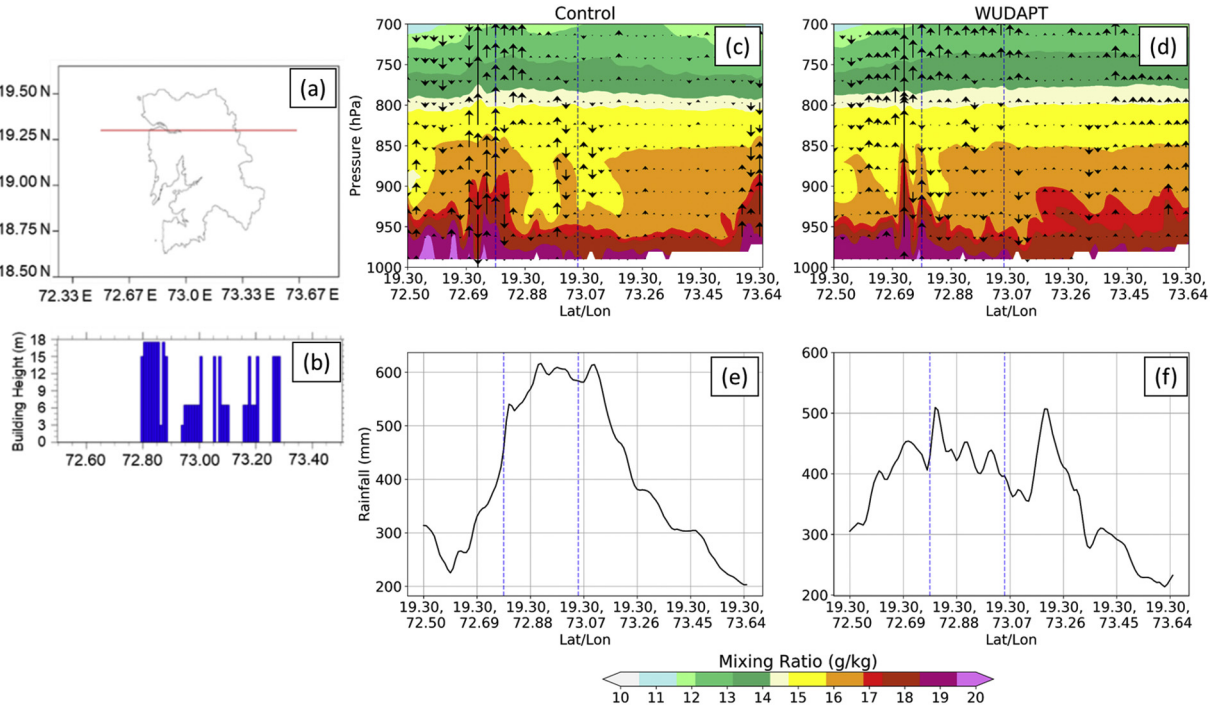


Fig. 8. WRF simulated fields for 1430 LT 28 Aug 2017 corresponding to a cross-section shown using the red line in (a), the corresponding building heights are shown in (b). The cross-section of vertical wind velocity overlaying mixing ratio for Control and WUDAPT simulation is shown in (c) and (d), the corresponding spatial variation in the rainfall is shown in (e) and (f), respectively. (For interpretation of the references to colour in this figure legend, the reader is referred to the web version of this article.)

Eqs. (1) and (2)). There is also variability introduced in the thermal properties of the building material, and urban fractions within the urban grids as compared to the Control. These changes in the surface characteristics and the mesoscale variability clearly affected the environment within the urban canyon, and the region above it leading to mesoscale changes in the simulated moisture and wind fields within the boundary layer, as also seen in Fig. 8(c-d).

Fig. 9 shows the virtual potential temperature (T_v) sounding up to 850 mb. The observations show a slightly unstable environment over the urban region in the 00Z profile, which is likely due to the mechanical mixing within urban canopy processes.

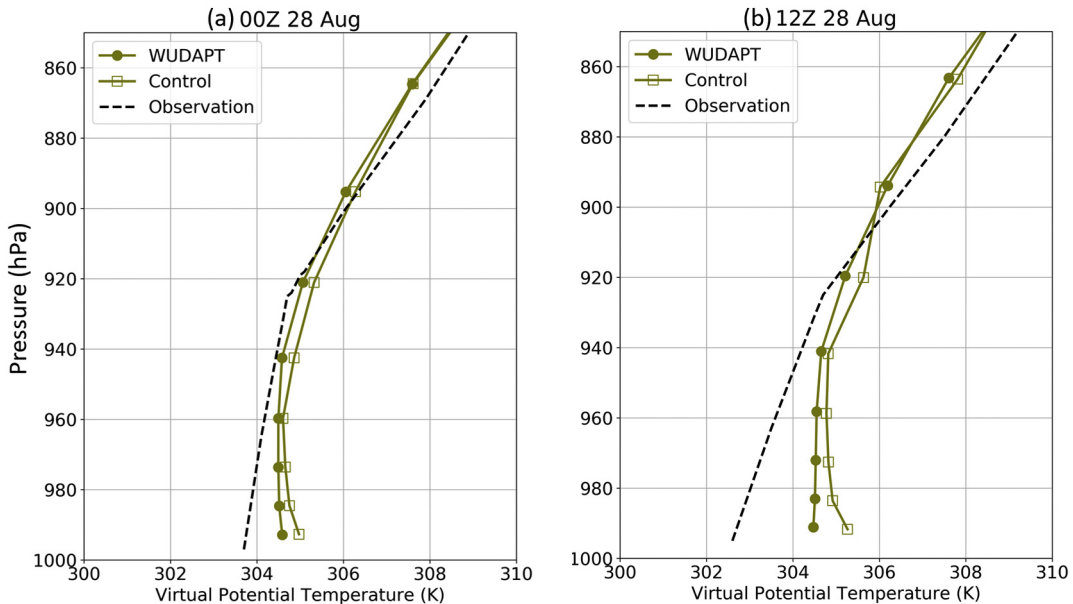


Fig. 9. Virtual potential temperature sounding at the Santacruz airport, Mumbai valid (a) 00Z (0530 LT), and (b) 12Z (1730 LT) on 28 August.

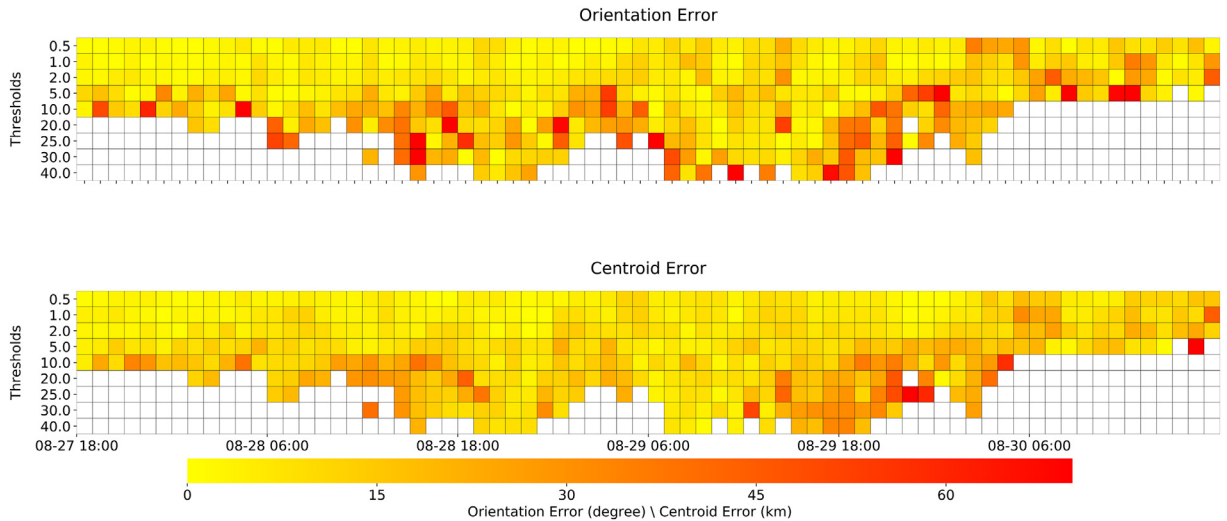


Fig. 10. Orientation and centroid errors for different rainfall thresholds calculated for Control and WUDAPT runs from MODE.

Interestingly, similar slightly unstable conditions were simulated with the WUDAPT run, while the Control simulated a stable surface environment, along with an inversion layer around 960 mb. The 12Z profile showed slightly unstable profile in the observation with an inversion around 925 mb. The simulated T_v profile for the WUDAPT run is relatively closer to the observations but simulated a near-neutral surface, while the Control simulates a slightly stable environment. Thus, the consideration of WUDAPT LCZ appeared to help simulate the turbulence and thermodynamic characteristics that helped represent the stability conditions that were relatively consistent with the observations. This was also noted in other convective measures such as CAPE and CIN values when comparing the observations, and the paired model runs. The morning profile showed a convective monsoonal setting with a CAPE value of 1058 J/kg from the observations, and the WUDAPT and Control simulated 832 J/kg and 55.9 J/kg, respectively. For the afternoon, the observed CAPE was 275.5 J/kg, possibly because of the intense rainfall, and the WUDAPT and Control simulated values were 250.5 J/kg and 296.9 J/kg respectively.

The rainfall fields from Control and WUDAPT simulations were compared using the MODE framework. Fig. 10 shows the orientation and centroid errors for different thresholds and timesteps. For rainfall thresholds corresponding to 0.5, 1.0, and 2.0 mm, there were insignificant changes in the centroid and orientation errors which grew with the model simulation period. The different rainfall thresholds typically show a difference of 15 km, with some extremes for high rainfall rates being off by about 30 km or more for centroid errors. The orientation or angle error (differences) of 80 degrees between the objects was also noted for the Control versus WUDAPT runs. For the smaller or low-intensity rainfall values (up to 10 mm), the two model runs had broadly similar results. As the rainfall amounts and rain rate increased the regions of heavy rains were separated in the simulation on an average by about 15–30 km (in terms of the centroid distance). There was also a difference in the manner in which the rainfall pattern extended with an

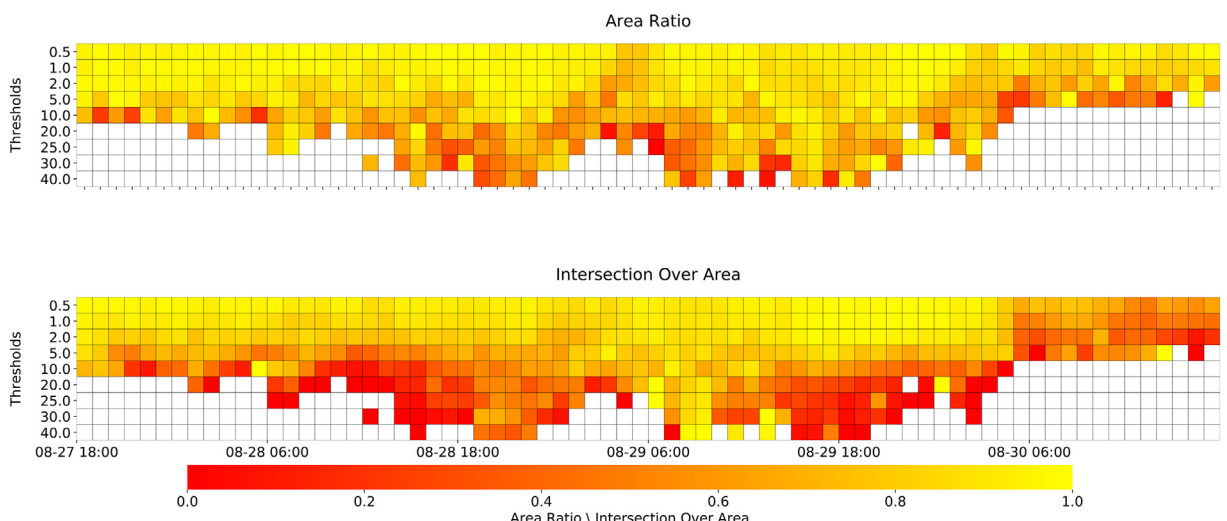


Fig. 11. Same as Fig. 10 but for area ratio and intersection over the area for different rainfall thresholds.

orientation difference of about 10–15 degrees for majority of the rainfall thresholds and even off by 45 degrees in extreme cases. Interestingly, the WUDAPT and Control simulated wind profile at Santacruz IMD observational site exhibited directional difference within the boundary layer for the 0Z and 12Z profile (WUDAPT fields being more north-northwesterly versus Control which was more westerly, not shown).

[Fig. 11](#) shows that as the rainfall threshold increased the differences (errors) in the rainfall area ratio and intersection over area also increased. In particular, for thresholds greater than 5 mm, the area ratio field showed considerable differences, indicating the location of rainfall peaks were simulated at different locations on an average. The resulting changes in the simulation of rainfall peaks, translated into the overall model performance across the domain. These results together highlight the need for the inclusion of LCZs information for heavy rainfall simulations over urban areas.

10. Additional events

Results for the three additional very heavy rains events across Mumbai are discussed next. The methodology was similar as detailed for the previous event. Results for the three events are summarized in [Fig. 12](#). Generally, the WUDAPT results are closer to the observed rainfall than the Control run, thus, reducing the bias from the Control simulations. Additional spatial accumulative plots for the three events are presented as supplementary information ([Fig. A.1–A.3](#)). The results are broadly similar and hence not discussed in detail; however following salient features emerge: (i) for the 2013 event ([Fig. A.1](#)), WUDAPT results lead to a more wider spatial variability with a reduction in the rainfall over the city and an increase in the surrounding area; (ii) the difference in the simulated rainfall fields from the paired runs is typically up to more than 100 mm, and (iii) the location of heavy rainfall pockets shows notable difference as well. The results thus further demonstrate that providing additional urban information helped reduce the bias in case of heavy rainfall simulation. Indeed, the results do not show consistent improvements and there was at least one case, such as the 2013 very heavy rain event, for which the WRF performance does not show marked improvements with respect to WUDAPT. This is particularly noted in terms of the spatial rainfall patterns (even though the average cumulative rainfall was relatively well simulated in WUDAPT as compared to Control).

11. Discussion and conclusions

This was the first study to investigate the impact of using WUDAPT based LCZ urban classification for the simulation of rainfall events over an urban area using WRF. The results based on simulations of four different very heavy rain events over Mumbai (for four different monsoon years), highlighted the enhancements in the WRF model's ability to simulate the rainfall processes when the WUDAPT urban LCZ data were used within the land model.

The model performance showed improvements in the cumulative rainfall estimates with WUDAPT as compared to the Control for each of the four cases. The changes in the spatial patterns due to the inclusion of WUDAPT data notably contributed to the overall rainfall occurrence over the urban area. In case of the 2017 very heavy rain event, the difference in the accumulated rainfall amounts simulated between the paired runs was over 300 mm. These changes in the rainfall distribution and quantity are the result of changes in the urban dynamics and micro/mesoscale convergence/divergence zones within the urban boundary layer.

The LCZ based urban classification helped in providing information to the model that is based on features such as building height, building distribution, open surfaces, and other thermal parameters. Thus the WUDAPT LCZ fields introduced mesoscale heterogeneity in morphological characteristics of the city, which in turn contributed to the changes in the surface turbulence and boundary layer features over the urban area. For example, the vertical winds covaried with the storm attributes and were found to have distinctly different structures due to the incorporation of urban morphological information implicit within the LCZs. The WUDAPT LCZ fields helped capture the microscale feedbacks that appear to organize and impact the mesoscale convergence/divergence, and convection fields in the WRF model.

The MODE analysis was found to be a useful tool for developing a more detailed assessment of the impact of the model runs and the impact on urban rainfall. Results indicated that rainfall values higher than 10 mm/h were affected more when the WUDAPT LCZ data was considered in the WRF runs. The consideration of WUDAPT dataset in the model also, as feedback, led to an increase in lead time and changes in the centroid, and the orientation of the objects for each of the threshold considered.

Thus, while the results indicate the WUDAPT LCZ fields can improve the simulation of heavy rain processes in the model, there are notable challenges related to integrating WUDAPT LCZs in the WRF runs. The first relates to the development of the classification of the LCZs, which is dependent on the personal experience of the city and generating a training dataset. To that end, a strategic, coordinated effort is underway as part of India's National Network Program on Urban Climate ([Gupta et al., 2018](#)). As a part of that program, WUDAPT maps of more than 100 Indian cities have been created. Beyond the creation of LCZ/WUDAPT maps, the other notable challenge is to have better representative database for urban parameters required for the atmospheric models that are not readily available at present. The uncertainties related to the LCZ classification is another caveat that will need to be addressed by combining the various satellite products and incorporating a collective consensus with the training datasets. Therefore, one possible way forward would be to develop a guided LCZ and morphological parameters generation for the cities.

Overall, the results, from dynamical perspective, as well as quantitative statistical metric, consistently and significantly highlighted the improvements in the WRF rainfall simulations by using WUDAPT LCZs. The improvements with respect to rainfall locations were not consistent and varied depending on the event, and requires further investigation in different cities. Thus, while the overall results and findings regarding the positive impact of incorporating WUDAPT within WRF for simulating heavy rainfall processes are robust, the transferability and generality of the results need to be considered by additional studies over different regions and by studying

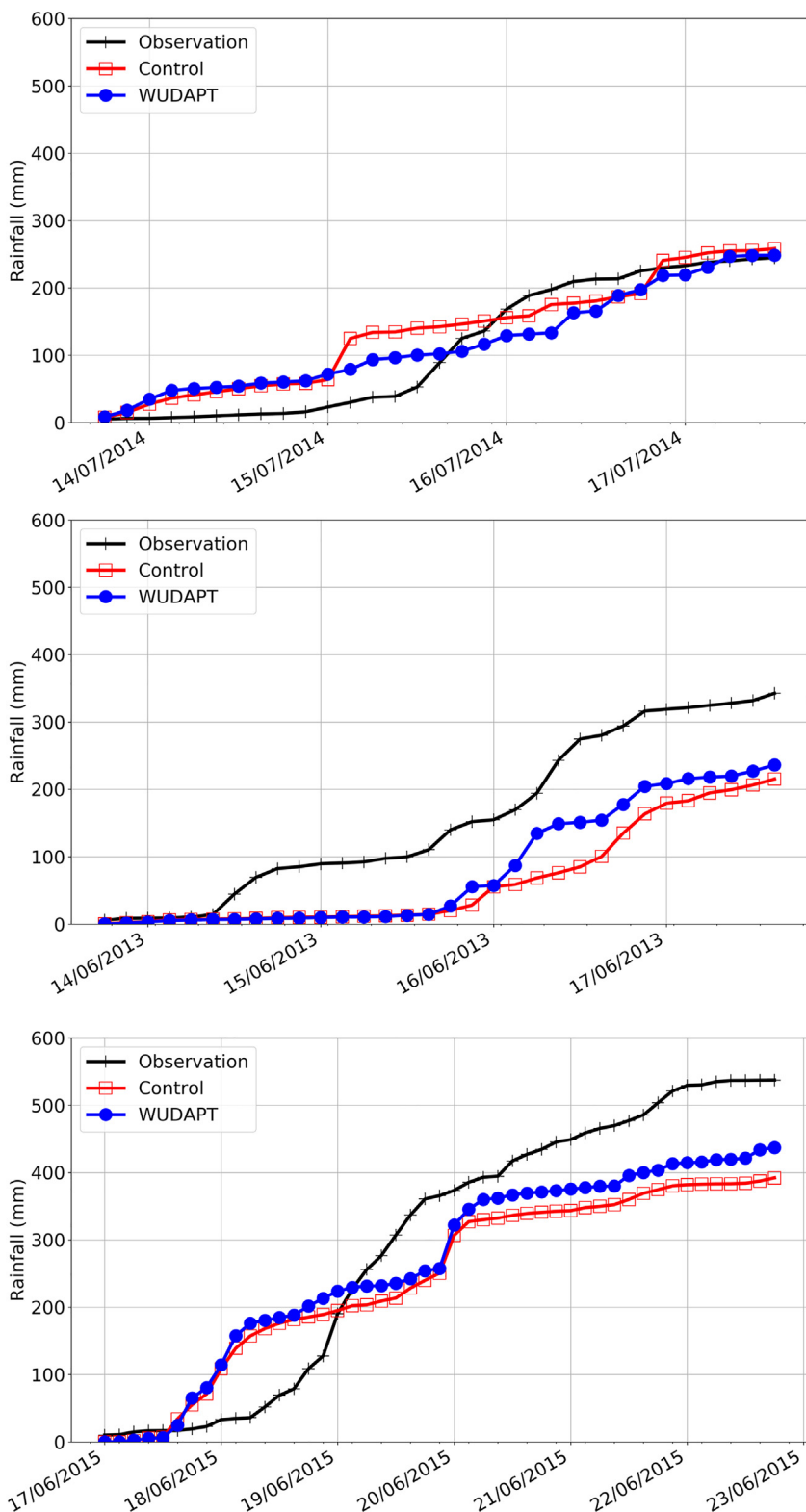


Fig. 12. Cumulative rainfall from Observed (green), Control (red), and WUDAPT (blue) simulations for the 2013 (top), 2014 (middle), and 2015 (bottom) very heavy rain events. (For interpretation of the references to colour in this figure legend, the reader is referred to the web version of this article.)

more events in future studies.

As an overarching conclusion, the study results provide positive incentive for developing detailed, urban morphological information for numerical weather prediction (NWP) models for enhancing meteorological forecasts for high impact urban weather events. The findings from this study can benefit the broader urban modeling community by extending the analysis to the other cities in different geographical settings, and is currently underway.

Declaration of Competing Interest

None.

Acknowledgement

This work benefitted in part through, Project MoES/PAMC/H&C/36/2013-PC-II from the Ministry of Earth Sciences, India; Department of Science & Technology (SPLICE - Climate Change Programme), India, Project DST/CCP/CoE/140/2018, Grant: 10013072 (UC ID: 18192442); US National Science FoundationOAC-1835739, AGS-1522492, USDA Hatch Project 1007699. The lead author acknowledges the SERB Overseas Visiting Doctoral Fellowship for a 1-year research visit to Purdue University.

Appendix A. Supplementary data

Supplementary data to this article can be found online at <https://doi.org/10.1016/j.ulim.2020.100616>.

References

- UN, 2018. World Urbanization Prospects 2018. (United Nations).
- Angel, S., Blei, A., Parent, J., Lamson-Hall, P., Sánchez, N.G., Civco, D.L., Lei, R.Q., Thom, K., 2015. Atlas of urban expansion—2016 edition. In: New York: The NYU Urbanization Project, Cambridge MA: The Lincoln Institute of Land Policy, and Nairobi. UN Habitat, Kenya.
- Bartesaghi Koc, C., Osmond, P., Peters, A., Irger, M., 2017. Mapping local climate zones for urban morphology classification based on airborne remote sensing data. 2017 Joint Urban Remote Sens. Event (JURSE) 1–4. <https://doi.org/10.1109/JURSE.2017.7924611>.
- Bechtel, B., Daneke, C., 2012. Classification of local climate zones based on multiple earth observation data. IEEE J. Select. Top. Appl. Earth Observ. Remote Sens. 5, 1191–1202. <https://doi.org/10.1109/JSTARS.2012.2189873>.
- Bechtel, B., Alexander, P., Böhner, J., Ching, J., Conrad, O., Feddema, J., Mills, G., See, L., Stewart, I., 2015. Mapping local climate zones for a worldwide database of the form and function of cities. ISPRS Int. J. Geo Inf. 4, 199–219.
- Bechtel, B., See, L., Mills, G., Foley, M., 2016. Classification of local climate zones using SAR and multispectral data in an arid environment. IEEE J. Select. Top. Appl. Earth Observ. Remote Sens. 9, 3097–3105. <https://doi.org/10.1109/JSTARS.2016.2531420>.
- Bossard, M., Feranec, J., Otahel, J., 2000. CORINE Land Cover Technical Guide: Addendum 2000. European Environment Agency, Copenhagen.
- Bougeault, P., Lacarrere, P., 1989. Parameterization of orography-induced turbulence in a Mesobeta-scale model. Mon. Weather Rev. 117, 1872–1890. [https://doi.org/10.1175/1520-0493\(1989\)117<1872:POQITI>2.0.CO;2](https://doi.org/10.1175/1520-0493(1989)117<1872:POQITI>2.0.CO;2).
- Brousse, O., Martilli, A., Foley, M., Mills, G., Bechtel, B., 2016. WUDAPT, an efficient land use producing data tool for mesoscale models? Integration of urban LCZ in WRF over Madrid. Urban Clim. 17, 116–134. <https://doi.org/10.1016/j.ulim.2016.04.001>. (arXiv:arXiv:1011.1669v3).
- Brousse, O., Georganos, S., Demuzere, M., Vanhuyse, S., Wouters, H., Wolff, E., Linard, C., Nicole, P.-M., Dujardin, S., 2019. Using local climate zones in sub-saharan africa to tackle urban health issues. Urban Clim. 27, 227–242.
- Cai, M., Ren, C., Xu, Y., 2017. Investigating the relationship between local climate zone and land surface temperature. 2017 Joint Urban Remote Sens. Event (JURSE) 1–4. <https://doi.org/10.1109/JURSE.2017.7924622>.
- Cassola, F., Ferrari, F., Mazzino, A., 2015. Numerical simulations of mediterranean heavy precipitation events with the wrf model: A verification exercise using different approaches. Atmos. Res. 164, 210–225.
- Chang, H.-I., Kumar, A., Niyogi, D., Mohanty, U., Chen, F., Dudhia, J., 2009. The role of land surface processes on the mesoscale simulation of the July 26, 2005 heavy rain event over Mumbai, India. Glob. Planet. Chang. 67, 87–103.
- Chawla, I., Osuri, K.K., Mujumdar, P.P., Niyogi, D., 2018. Assessment of the weather research and forecasting (WRF) model for simulation of extreme rainfall events in the upper Ganga Basin. Hydrol. Earth Syst. Sci. 22.
- Chen, F., Kusaka, H., Bornstein, R., Ching, J., Grimmond, C.S.B., Grossman-Clarke, S., Loridan, T., Manning, K.W., Martilli, A., Miao, S., Sailor, D., Salamanca, F.P., Taha, H., Tewari, M., Wang, X., Wyszogrodzki, A.A., Zhang, C., 2011. The integrated WRF/urban modelling system: development, evaluation, and applications to urban environmental problems. Int. J. Climatol. 31, 273–288. <https://doi.org/10.1002/joc.2158>.
- Ching, J., Mills, G., Bechtel, B., See, L., Feddema, J., Wang, X., Ren, C., Brorousse, O., Martilli, A., Neophytou, M., Mouzourides, P., Stewart, I., Hanna, A., Ng, E., Foley, M., Alexander, P., Aliaga, D., Niyogi, D., Shreevastava, A., Bhalachandran, P., Masson, V., Hidalgo, J., Fung, J., Andrade, M., Baklanov, A., Dai, W., Milcinski, G., Demuzere, M., Brunsell, N., Pesaresi, M., Miao, S., Mu, Q., Chen, F., Theeuwes, N., 2018. WUDAPT: an urban weather, climate, and environmental modeling infrastructure for the anthropocene. Bull. Am. Meteorol. Soc. 99, 1907–1924. <https://doi.org/10.1175/BAMS-D-16-0236.1>.
- Clark, A.J., Bullock, R.G., Jensen, T.L., Xue, M., Kong, F., 2014. Application of object-based time-domain diagnostics for tracking precipitation systems in convection-allowing models. Weather Forecast. 29, 517–542.
- Conrad, O., Bechtel, B., Bock, M., Dietrich, H., Fischer, E., Gerlitz, L., Wehberg, J., Wichmann, V., Böhner, J., 2015. System for automated geoscientific analyses (SAGA) v. 2.1. 4. Geosci. Model Dev. 8, 1991–2007.
- Davis, C.A., Brown, B.G., Bullock, R., Halley-Gotway, J., 2009. The method for object-based diagnostic evaluation (MODE) applied to numerical forecasts from the 2005 NSSL/SPC spring program. Weather Forecast. 24, 1252–1267.
- Dhiman, R., VishnuRadhan, R., Eldho, T., Inamdar, A., 2019. Flood risk and adaptation in indian coastal cities: recent scenarios. Appl Water Sci 9, 5.
- Dudhia, J., 1989. Numerical study of convection observed during the winter monsoon experiment using a mesoscale two-dimensional model. J. Atmos. Sci. 46, 3077–3107. [https://doi.org/10.1175/1520-0469\(1989\)046<3077:NSOCOD>2.0.CO;2](https://doi.org/10.1175/1520-0469(1989)046<3077:NSOCOD>2.0.CO;2).
- Dutta, D., Routray, A., Kumar, D.P., George, J.P., Singh, V., 2019. Simulation of a heavy rainfall event during southwest monsoon using high-resolution NCUM-modeling system: a case study. Meteorol. Atmos. Phys. 131, 1035–1054.
- Feddema, J., Mills, G., Ching, J., 2015. Demonstrating the added value of wudapt for urban climate modelling. In: 9th International Conference on Urban Climate.
- Gál, T., Bechtel, B., Unger, J., 2015. Comparison of two different Local Climate Zone mapping methods. In: 9th International Conference on Urban Climate.
- Geletič, J., Lehnhert, M., 2016. GIS-based delineation of local climate zones: the case of medium-sized central European cities. Moravian Geogr. Rep. 24, 2–12. <https://doi.org/10.1515/mgr-2016-0012>.
- Glotfelty, T., Tewari, M., Sampson, K., Duda, M., Chen, F., Ching, J., 2013. NUDAPT 44 documentation. National Center for Atmospheric Research Research

- Applications Laboratory.**
- Grell, G.A., Dévényi, D., 2002. A generalized approach to parameterizing convection combining ensemble and data assimilation techniques. *Geophys. Res. Lett.* 29, <https://doi.org/10.1029/2002GL015311>. (38–1–38–4).
- Grossman, R.L., Durran, D.R., 1984. Interaction of low-level flow with the western Ghat mountains and offshore convection in the summer monsoon. *Mon. Weather Rev.* 112, 652–672.
- Gupta, A., Niyogi, D., Mohanty, U.C., 2018. National Network Research Program on urban climate for India. In: 10th International Conference on Urban Climate/14th Symposium on the Urban Environment.
- IMD, 2019a. IMD Terminologies and Glossary. <http://www.imdpune.gov.in/Weather/Reports/glossary.pdf>, Accessed date: 14 April 2019.
- IMD, 2019b. Mumbai City Climatology. <http://city.imd.gov.in/citywx/extreme/APR/mumbai2.htm>, Accessed date: 14 April 2019.
- Jenamani, R.K., Bhan, S., Kalsi, S., 2006. Observational/forecasting aspects of the meteorological event that caused a record highest rainfall in Mumbai. *Curr. Sci.* 1344–1362.
- Kaloustian, N., Bechtel, B., 2016. Local climatic zoning and urban heat island in Beirut. *Proc. Eng.* 169, 216–223. <https://doi.org/10.1016/j.proeng.2016.10.026>.
- Kotharkar, R., Bagade, A., 2018. Evaluating urban heat island in the critical local climate zones of an Indian city. *Landscape. Urban Plan.* 169, 92–104.
- Kumar, A., Dudhia, J., Rotunno, R., Niyogi, D., Mohanty, U., 2008. Analysis of the 26 July 2005 heavy rain event over Mumbai, India using the Weather Research and Forecasting (WRF) model. *Q. J. R. Meteorol. Soc.* 134, 1897–1910.
- Leconte, F., Bouyer, J., Claverie, R., Pétrissans, M., 2015. Using local climate zone scheme for UHI assessment: evaluation of the method using mobile measurements. *Build. Environ.* 83, 39–49.
- Lei, M., Niyogi, D., Kishtawal, C., Pielke Sr., R., Beltrán-Przekurat, A., Nobis, T., Vaidya, S., 2008. Effect of explicit urban land surface representation on the simulation of the 26 July 2005 heavy rain event over Mumbai, India. *Atmos. Chem. Phys.* 8, 5975–5995.
- Lorenz, J.M., Kronenberg, R., Bernhofer, C., Niyogi, D., 2019. Urban rainfall modification: observational climatology over Berlin, Germany. *J. Geophys. Res.-Atmos.* 124, 731–746.
- Martilli, A., Clappier, A., Rotach, M.W., 2002. An urban surface exchange parameterisation for mesoscale models. *Bound.-Layer Meteorol.* 104, 261–304.
- Mlawer, E.J., Taubman, S.J., Brown, P.D., Iacono, M.J., Clough, S.A., 1997. Radiative transfer for inhomogeneous atmospheres: RRTM, a validated correlated-k model for the longwave. *J. Geophys. Res.* 102, 16663. <https://doi.org/10.1029/97JD00237>.
- Niyogi, D., 2017. From urban climatology to climate proofing cities. In: EGU General Assembly Conference Abstracts. Volume 19. pp. 19634.
- Niyogi, D., Pyle, P., Lei, M., Arya, S.P., Kishtawal, C.M., Shepherd, M., Chen, F., Wolfe, B., 2011. Urban modification of thunderstorms: an observational storm climatology and model case study for the Indianapolis urban region. *J. Appl. Meteorol. Climatol.* 50, 1129–1144. <https://doi.org/10.1175/2010JAMC1836.1>.
- Patel, P., Ghosh, S., Kaginekar, A., Islam, S., Karmakar, S., 2019. Performance evaluation of WRF for extreme flood forecasts in a coastal urban environment. *Atmos. Res.* 223, 39–48. <https://doi.org/10.1016/j.atmosres.2019.03.005>.
- Patel, S., Ghosh, S., Mathew, M., Devanand, A., Karmakar, S., Niyogi, D., 2018. Increased spatial variability and intensification of extreme monsoon rainfall due to urbanization. *Sci. Rep.* 8, 3918. <https://doi.org/10.1038/s41598-018-22322-9>.
- Rao, Y.R., Hatwar, H., Salah, A.K., Sudhakar, Y., 2007. An experiment using the high resolution Eta and WRF models to forecast heavy precipitation over India. *Pure Appl. Geophys.* 164, 1593–1615.
- Routray, A., Mohanty, U., Niyogi, D., Rizvi, S., Osuri, K.K., 2010. Simulation of heavy rainfall events over Indian monsoon region using WRF-3DVAR data assimilation system. *Meteorol. Atmos. Phys.* 106, 107–125.
- Salamanca, F., Martilli, A., 2010. A new building energy model coupled with an urban canopy parameterization for urban climate simulations-part II. Validation with one dimension off-line simulations. *Theor. Appl. Climatol.* 99, 345–356. <https://doi.org/10.1007/s00704-009-0143-8>.
- Salamanca, F., Krpo, A., Martilli, A., Clappier, A., 2010. A new building energy model coupled with an urban canopy parameterization for urban climate simulations-part I. formulation, verification, and sensitivity analysis of the model. *Theor. Appl. Climatol.* 99, 331–344. <https://doi.org/10.1007/s00704-009-0142-9>.
- Samsonov, T., Trigub, K., 2017. Towards computation of urban local climate zones (LCZ) from openstreetmap data. In: Proceedings of the 14th International Conference on GeoComputation, 4th–7th September 2017. Leeds, UK, pp. 1–9.
- Skamarock, W., Klemp, J., Dudhia, J., Gill, D., Barker, D., Duda, M., Huang, X.-Y., Wang, W., Powers, J., 2008. A description of the advanced research WRF version 3. In: Technical Report June National Center for Atmospheric Research Boulder, Colorado, USA, <https://doi.org/10.5065/D6DZ069T>.
- Stewart, I.D., Oke, T.R., 2012. Local climate zones for urban temperature studies. *Bull. Am. Meteorol. Soc.* 93, 1879–1900. <https://doi.org/10.1175/BAMS-D-11-00019.1>.
- Story, M., Congalton, R.G., 1986. Accuracy assessment: a user's perspective. *Photogramm. Eng. Remote. Sens.* 52, 397–399.
- Tewari, M., Chen, F., Wang, W., Dudhia, J., LeMone, M., Mitchell, K., Ek, M., Gayno, G., Wegiel, J., Cuenca, R., 2004. Implementation and verification of the unified noah land surface model in the wrf model. In: 20th Conference on Weather Analysis and Forecasting/16th Conference on Numerical Weather Prediction.
- Thomas, G., Sherin, A., Ansar, S., Zachariah, E., 2014. Analysis of urban heat island in Kochi, India, using a modified local climate zone classification. *Procedia Environ. Sci.* 21, 3–13.
- Thompson, G., Field, P.R., Rasmussen, R.M., Hall, W.D., 2008. Explicit forecasts of winter precipitation using an improved bulk microphysics scheme. Part II: implementation of a new snow parameterization. *Mon. Weather Rev.* 136, 5095–5115. <https://doi.org/10.1175/2008MWR2387.1>. (arXiv:0402594v3).
- Vaidya, S., Kulkarni, J., 2007. Simulation of heavy precipitation over Santacruz, Mumbai on 26 July 2005, using mesoscale model. *Meteorol. Atmos. Phys.* 98, 55–66.
- Verdonck, M.-L., Okujeni, A., van der Linden, S., Demuzere, M., De Wulf, R., Van Coillie, F., 2017. Influence of neighbourhood information on 'Local Climate Zone' mapping in heterogeneous cities. *Int. J. Appl. Earth Obs. Geoinf.* 62, 102–113. <https://doi.org/10.1016/j.jag.2017.05.017>.
- Wang, R., Ren, C., Xu, Y., Lau, K.K.L., Shi, Y., 2018. Mapping the local climate zones of urban areas by GIS-based and WUDAPT methods: A case study of Hong Kong. *Urban Clim.* 24, 567–576. <https://doi.org/10.1016/j.uclim.2017.10.001>.
- Wittke, S., Karila, K., Puttonen, E., Hellsten, A., Auvinen, M., Karjalainen, M., 2017. Extracting urban morphology for atmospheric modeling from multispectral and SAR satellite imagery. *Int. Arch. Photogr. Remote Sens. Spatial Inform. Sci. ISPRS Archiv.* 42, 425–431. <https://doi.org/10.5194/isprs-archives-XLII-1-W1-425-2017>.
- Wouters, H., Demuzere, M., Blahak, U., Fortuniak, K., Maiheu, B., Camps, J., Tielemans, D., van Lipzig, N.P.M., 2016. The efficient urban canopy dependency parametrization (SURY) v1.0 for atmospheric modelling: description and application with the COSMO-CLM model for a Belgian summer. *Geosci. Model Dev.* 9, 3027–3054. <https://www.geosci-model-dev.net/9/3027/2016/> <https://doi.org/10.5194/gmd-9-3027-2016>.
- Xu, Y., Ren, C., Cai, M., Edward, N.Y.Y., Wu, T., 2017. Classification of local climate zones using ASTER and Landsat data for high-density cities. *IEEE J. Select. Top. Appl. Earth Observ. Remote Sens.* 10, 3397–3405. <https://doi.org/10.1109/JSTARS.2017.2683484>.
- Yokoya, N., Ghamisi, P., Xia, J., 2017. Multimodal, multitemporal, and multisource global data fusion for local climate zones classification based on ensemble learning. In: 2017 IEEE International Geoscience and Remote Sensing Symposium (IGARSS). IEEE, pp. 1197–1200.